Characterizing the Assembly of the Sup35 Yeast Prion Fragment, GNNQQNY: Structural Changes Accompany a Fiber-to-Crystal Switch

Karen E. Marshall,[†] Matthew R. Hicks,[‡§] Thomas L. Williams,[†] Søren Vrønning Hoffmann,[¶] Alison Rodger,[‡] Timothy R. Dafforn,[§] and Louise C. Serpell[†*]

[†]Department of Biochemistry, School of Life Sciences, University of Sussex, Falmer, BN1 9QG United Kingdom; [‡]Department of Chemistry, University of Warwick, Coventry, CV4 7AL United Kingdom; [§]School of Biosciences, University of Birmingham, Birmingham, B15 2TT United Kingdom; and [¶]Institute for Storage Ring Facilities, Aarhus University, Aarhus, DK-8000 Denmark

ABSTRACT Amyloid-like fibrils can be formed by many different proteins and peptides. The structural characteristics of these fibers are very similar to those of amyloid fibrils that are deposited in a number of protein misfolding diseases, including Alzheimer's disease and the transmissible spongiform encephalopathies. The elucidation of two crystal structures from an amyloid-like fibril-forming fragment of the yeast prion, Sup35, with sequence GNNQQNY, has contributed to knowledge regarding side-chain packing of amyloid-forming peptides. Both structures share a cross-β steric zipper arrangement but vary in the packing of the peptide, particularly in terms of the tyrosine residue. We investigated the fibrillar and crystalline structure and assembly of the GNNQQNY peptide using x-ray fiber diffraction, electron microscopy, intrinsic and quenched tyrosine fluorescence, and linear dichroism. Electron micrographs reveal that at concentrations between 0.5 and 10 mg/mL, fibers form initially, followed by crystals. Fluorescence studies suggest that the environment of the tyrosine residue changes as crystals form. This is corroborated by linear dichroism experiments that indicate a change in the orientation of the tyrosine residue over time, which suggests that a structural rearrangement occurs as the crystals form. Experimental x-ray diffraction patterns from fibers and crystals also suggest that these species are structurally distinct. A comparison of experimental and calculated diffraction patterns contributes to an understanding of the different arrangements accessed by the peptide.

INTRODUCTION

Many diseases, including Alzheimer's disease and the transmissible spongiform encephalopathies, involve the deposition of normally soluble protein in the form of amyloid fibrils, and this process is thought to be a key factor in their pathology (1). Amyloid is defined by a variety of criteria, including staining by the dye Congo Red and a long, unbranched appearance when viewed by electron microscopy (EM). There is strong evidence that amyloid has a structure known as cross-β (first observed in the egg stalk of the lacewing *Chrysopa* (2)), which shows characteristic reflections at 4.7 Å and 10–11 Å in x-ray fiber diffraction patterns arising from the hydrogen bonding between β-strands and the spacing between β-sheets, respectively (3,4). This characteristic cross-β pattern is also used as a diagnostic tool to identify amyloid fibrils (5). To understand how proteins misfold and assemble to form these well-ordered fibers, and to gain insight into how they may cause disease, detailed structural knowledge is required. To date, crystallization of full-length amyloid-forming peptides and proteins related to disease has not been possible, so structural information has been obtained by other methods, including solid-state NMR (6), cryo-EM (7–9), atomic force microscopy (10), and x-ray fiber diffraction (11). Recent advances have also been made using model systems comprised of short synthetic peptides, often fragments from proteins associated with disease (11,12). The structures of short peptides ($\leq$7 amino acids) that form amyloid fibers and microcrystals were recently solved by x-ray crystallography, and these structures share a ''steric zipper'' arrangement (13,14). The accumulation of these data has led to the definition of eight different classes of steric zipper that depend on the orientation of β-strands and β-sheets in relation to one another (14). One of these, the seven-residue peptide GNNQQNY, is a motif from the N-terminus of the yeast prion-like protein, Sup35. The role of Sup35 in its native state is to terminate translation in yeast, but it has also shown the ability to transmit its alternative conformation and take part in prion-like activity (15). GNNQQNY was previously shown to exhibit amyloid-forming properties similar to those of the full-length peptide (15), and, depending on the concentration and incubation time, this peptide can form both fibrils and microcrystals. However, the methods used to achieve these different species vary, and heterogeneous solutions are often produced (13,15–17). The concentrations required to form fibrils in particular vary greatly, and their presence has been reported at concentrations as low as 0.3 mg/mL (13). Conversely, Diaz-Avalos et al. (16) reported that neither fibers nor crystals form at $\leq$5 mg/mL, even after prolonged periods, and that much higher concentrations are required (>20 mg/mL) to form fibers, in agreement with other groups (17). Initial studies using a concentration of 10 mg/mL produced crystals that were subjected to powder and electron diffraction (15,16). Further work produced larger crystals that were of sufficient size for structure determination by x-ray

Submitted August 12, 2009, and accepted for publication October 15, 2009.

*Correspondence: L.C.Serpell@sussex.ac.uk

Editor: Kathleen B. Hall.

0006-3495/10/01/0330/9 $2.00

doi: 10.1016/j.bpj.2009.10.020

crystallography. Two crystal structures have been solved that both contain pairs of parallel β-sheets with side chains interdigitating in an anhydrous steric zipper (13,14). However, the two structures differ considerably in the packing of the peptide, crystallizing in monoclinic (1yjp.pdb) (13) or orthorhombic (2omm.pdb) (14) forms (see Fig. S1 in the Supporting Material). Solid-state NMR measurements carried out on the two different crystal forms corroborate previous findings that the two forms are similar and share a cross-β arrangement, with the main differences being in the environment of the tyrosine residue (17). In the monoclinic form, the side chain appears to be immobile and responsible for stabilizing the interaction between pairs of sheets across the wet interface via π-π interactions, whereas in the orthorhombic form it has no such role (17). Furthermore, solid-state NMR experiments on fibrillar forms of GNNQQNY show similarities to the orthorhombic form of the crystals, suggesting that the mobile tyrosine residue is responsible for polymorphisms within fibrillar structures (17).

The importance of aromatic interactions in amyloid formation was discussed previously (18), which would imply that the tyrosine residue of GNNQQNY is important for fibril formation and/or the overall stability of the fiber. Nelson et al. (13) suggested that fibril formation proceeds initially by the formation of a nucleus consisting of β-sheets held together by side-chain interactions. The stability of such a nucleus has been verified by molecular-dynamics simulations on GNNQQNY (19), indicating that interactions in the steric zipper by even a limited number of β-strands may be responsible for the overall stability of the fiber (19). It is conceivable that alternative structures could arise from different bonding patterns between side chains, as evidenced by the two crystal forms (13,14,20). It is unclear at present whether either or any of these crystal structures truly represent the structure of the fibril, or whether it takes on some entirely different arrangement.

Most of the work on GNNQQNY to date has focused on structural characterization of the end-point species formed after fibrillization and crystallization, and has uncovered variations in morphology. In this work we investigated the actual assembly process using a number of biophysical techniques to gain insight into the pathways by which fibers and crystals form. The role of the tyrosine residue in driving fibril or crystal formation is of particular interest. Measurement of intrinsic and quenched tyrosine fluorescence can provide information regarding the environment of the tyrosine residue, and was previously used to follow structural changes that occur during amyloid fibril formation (21,22). Similarly, circular dichroism (CD) is classically used to obtain information on protein secondary structure and can report on these changes as fibrillization proceeds, typically from random coil or folded native structures to β-sheet-containing species (23). However, it is known that aromatic residues can contribute significantly to CD spectra in both the near- and far-UV regions (24,25). Furthermore, aromatic residues in close proximity can undergo coupling of their transitions and intensify these contributions, which can complicate data interpretation. In this study, we used linear dichroism (LD) to obtain information on both the secondary structure and the orientation of chromophores within the larger structure (see Rodger and Nordén for an overview (26)). This method can give information regarding the orientation of the π-π^* transitions in the peptide bond of β-sheet structures that absorb light at ~195 nm. The sign of the LD signal at this wavelength therefore identifies the orientation of β-strands relative to a larger structure, in this case a peptide fiber. In addition, it is also possible to determine the orientation of aromatic side chains within peptide fibers. Furthermore, the LD signal can be measured in real time to follow the kinetic processes that occur during fiber formation, and to identify changes in backbone and aromatic side-chain orientation that occur during this process. Fiber diffraction analysis of the different species that form over time can also reveal how the morphology changes as assembly proceeds.

Because the peptide GNNQQNY is one of the few amyloidogenic peptides that have been characterized structurally by x-ray crystallography, it provides an excellent model system for further investigation into the process of fibrillization. In this work, we investigate the assembly and accompanying structural changes that occur in the formation of GNNQQNY fibers and crystals. Fluorescence studies indicate that the assembly process is accompanied by a change in the environment of the C-terminal tyrosine residue. This is correlated to morphological changes observed by EM that indicate a development of amyloid-like fibrils to larger crystalline assemblies. LD indicates that the orientation of the tyrosine residue is also altered with the assembly process. Finally, x-ray fiber diffraction of fibers and crystals indicates structural differences between these two morphological forms, and a comparison of the fiber patterns calculated from the two crystal forms suggests that whereas the crystals are consistent with the orthorhombic structure, the fibers may represent an alternative packing arrangement.

MATERIALS AND METHODS

Peptide synthesis and sample preparation

NH_3+-GNNQQNY-COO- was purchased from Pepceuticals (Biocity, Nottingham, UK) at >97% purity. Stock solutions were made up in Milli-Q (Millipore, Billerica, MA) 0.2 μm filtered water at concentrations of 2–3 mg/mL. The concentration was determined using a molar extinction coefficient of 1490 M^{-1} cm^{-1} and by measuring absorbance at a wavelength of 280 nm using an Eppendorf biophotometer (Eppendorf AG, Hamburg, Germany).

Electron microscopy

4 μL of solution were placed onto carbon-coated copper grids (Agar Scientific, Essex, UK), blotted, and then negatively stained with 4 μL of 2% uranyl acetate and blotted. The grid was allowed to air-dry before it was

examined in a Hitachi 7100 microscope (Hitachi, Germany) fitted with a Gatan Ultrascan 1000 CCD camera (Gatan, Abingdon, UK). Aliquots of samples were taken at various time points for each experiment. Measurements were made using ImageJ (27).

Tyrosine fluorescence

Immediately after the addition of water to obtain a final peptide concentration of 3 mg/mL, the samples were centrifuged at 13,000 rpm for 5 min to remove any preformed aggregates. Any pellet that formed was discarded. The samples were placed in a quartz cuvette (Starna, Essex, UK) with a 1 cm pathlength, and the fluorescence from tyrosine was monitored at various time points using a Varian Cary Eclipse fluorimeter (Varian, Oxford, UK) with an excitation wavelength of 278 nm. Fluorescence intensities at the peak of 305 nm were plotted against time. Excitation and emission slits were set to 5 and 10 nm, respectively. The scan rate was set to 600 nm/min with 1 nm data intervals and an averaging time of 0.1 s. Experiments were carried out in triplicate to confirm trends.

Acrylamide quenching

Samples were prepared as for the tyrosine fluorescence experiments, with identical fluorimeter settings. Quenching effects were observed on fibrils (time 0) and crystals (168 h). At each time point, acrylamide was titrated into the sample at increasing concentrations between 0.1 and 0.4 M, and a fluorescence reading was taken. A reading was also taken with no acrylamide present. The data were fitted to the Stern-Volmer equation, which is used to describe collisional quenching:

$$F_0/F = 1 + K_{SV}[Q],$$

where F_0 is the fluorescence intensity in the absence of acrylamide, F is the fluorescence intensity in the presence of acrylamide, Q is the concentration of acrylamide, and K_{SV} is the Stern-Volmer quenching constant (28). Linear plots of F_0/F against $[Q]$ gave K_{SV} values for fibrils and crystals; higher values indicate that the tyrosine is more easily quenched and therefore more solvent-accessible.

Linear dichroism

Peptide was preincubated for several weeks in water to enable the formation of crystals at a concentration of 2 mg/mL and was diluted to 0.2 mg/mL. Equilibrium LD measurements were performed on a Jasco J-815 spectropolarimeter (Great Dunmow, UK) from 350–180 nm with a bandwidth of 2 nm, scanning speed of 100 nm/min, response of 1 s, standard sensitivity, and data pitch of 0.2 nm. Alignment of the samples was achieved using a microvolume Couette cell with a rotation speed of 3000 rpm, which was built in-house (equivalent models are available from Kromatek, Great Dunmow, UK). Eight spectra were averaged and a water baseline spectrum was subtracted from this to account for the inherent LD signal of the system originating from the optics and the detector. LD spectra are reported in δ absorbance units.

For kinetics experiments, LD spectroscopy was performed on freshly solubilized peptide. The peptide was dissolved in water at a concentration of 2 mg/mL. Alignment was induced by using a microvolume Couette cell (Kromatek, Great Dunmow, UK) with a pathlength of 0.5 mm (29). Experiments were carried out on the UV1 beamline at the Synchrotron Radiation Facility ASTRID at the Institute for Storage Ring Facilities, Aarhus University (Aarhus, Denmark) and on a Jasco J-815 spectropolarimeter. ASTRID provided a much enhanced signal/noise ratio, which allowed the rapid scanning required for kinetic measurements of samples that inherently scatter light at low wavelengths, such as protein fibers. Spectra were measured between 180 nm and 350 nm at 1 nm steps using the low-energy grating of the UV1 beamline at a spectral resolution of ~1 nm. The beamline was set up as described previously (30). Spectra were measured at a cell rotation speed of 3000 rpm and a water baseline spectrum was subtracted from this to account for the inherent LD signal of the system originating from the optics and the detector. Synchrotron radiation spectra are reported in the output signal from the lock-in amplifier (in millivolts). In terms of δ absorbance units, 1 mV is ~6×10^{-4} Å.

X-ray fiber diffraction

A stock solution of peptide at 10 mg/mL was incubated at room temperature. At various time points, aliquots were taken to check for the presence of fibers, crystals, or a mixture of both using EM. For the samples containing fibers and a mixture of crystals and fibers, 20 μL of solution were placed between two wax-filled capillaries and allowed to air-dry at room temperature. Alternatively, the crystalline sample was placed into a siliconized 0.7 mm capillary tube, sealed with wax at one end, and allowed to dry over a few weeks at room temperature. The resulting sample was a disk in which the crystals were generally oriented across the capillary. The capillary containing the dried disk was sealed at the top end. The fiber or disk sample was placed on a goniometer head, and data were collected with the use of a Rigaku (Sevenoaks, UK) rotating anode (CuKα) and Raxis IV++ detector (Sevenoaks, UK), with a specimen-to-film distance of 160 mm or 250 mm.

X-ray diffraction simulation from coordinates

Diffraction patterns were calculated from model coordinates from 1yjp.pdb and 2omm.pdb using the published unit cell dimensions. This was done using the fiber diffraction analysis program Clearer (31), which generates fiber diffraction patterns from input structural coordinates, as previously described (31,32). The fiber axis was assigned to be parallel to the hydrogen-bonding direction of the coordinates, and the beam direction was perpendicular. The calculated diffraction pattern took into account the diffraction settings associated with the experimental data collection (specimen-to-detector distance, pixel size) to allow direct comparison between experimental and calculated diffraction patterns.

RESULTS

EM reveals that GNNQQNY forms fibers followed by crystals

At all concentrations between 0.5 and 10 mg/mL, electron micrographs show that immediately after dissolving in water, the peptide GNNQQNY forms fibrils that eventually develop to form crystalline assemblies, with very little or no fibrils present (data are shown only for a 3 mg/mL sample). Even at very low concentrations, some fibrillar material was observed at time ''zero'' (despite the attempted removal of preformed aggregates by centrifugation), although it was much less abundant, and the crystals that formed at later time points were generally smaller in width. The time it takes for these transitions to occur varies depending on the concentration, but after several days, in all cases only crystals were present. Fig. 1, *a–e*, shows electron micrographs of a 3 mg/mL sample of GNNQQNY at time 0, 3, 24, 72, and 192 h. At time 0 (Fig. 1 *a*) the fibrils show the long, unbranching appearance characteristic of amyloid. Individual fibrils are ~5–10 nm wide, and even at this stage there appears to be some lateral association of fibrils into ribbons of ~20–25 nm (denoted by * and shown in the inset of Fig. 1). By 3 h (Fig. 1 *b*) the average width of the ribbons increases to ~30–60 nm and there are far fewer smaller-width fibrils. Much larger crystalline species (~150–350 nm wide)

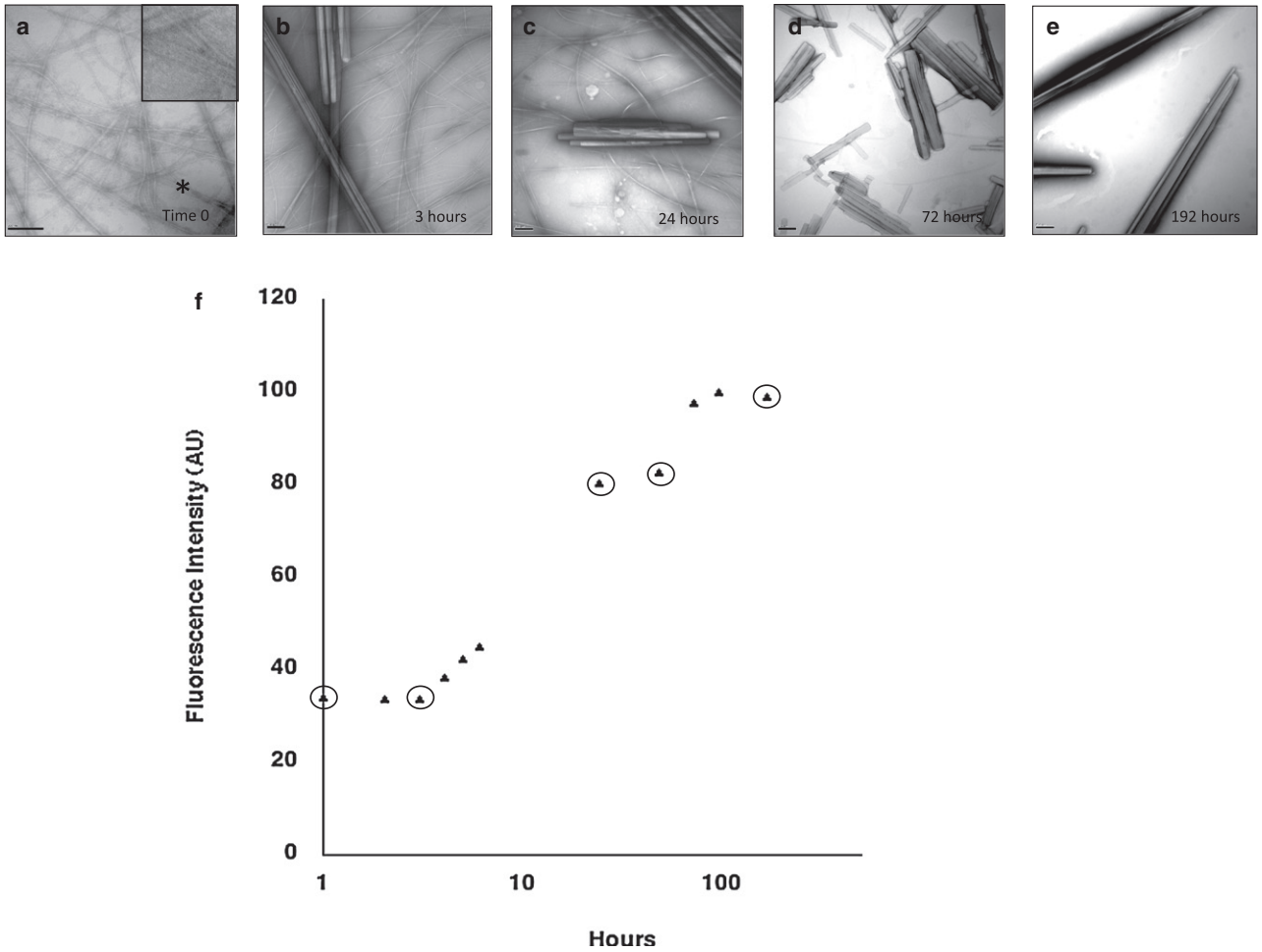

FIGURE 1 Changes in the morphology and tyrosine fluorescence of GNNQQNY over time. (*a–e*) EM images of GNNQQNY taken at various time points. Scale bars are 200 nm in all images. (*f*) Increase in tyrosine fluorescence intensity at 305 nm over time. Circled data points correspond to EM images shown in *a–e*.

are also present. At 24 h (Fig. 1 *c*) the average sizes are uniform but there are fewer fibrils or ribbons in the background, and by 72 h (Fig. 1 *d*) the fibrillar material has disappeared completely.

An increase in intrinsic tyrosine fluorescence correlates with the transition from fibers to crystals

Structural information obtained from previous crystallization and solid-state NMR experiments (13,14,17) suggests that tyrosine plays an important role in this assembly. We investigated this further using intrinsic fluorescence and quenching experiments. A representative concentration of 3 mg/mL was used to compare the morphological changes observed by EM with any changes in tyrosine fluorescence, which would indicate a change in the environment of the tyrosine residue. Fig. 1 *f* shows that the tyrosine fluorescence increases over time, with a lag phase up to 3 h, followed by an increase in intensity up to ~72 h, at which point the fluorescence intensity reaches a plateau. These changes correspond to the initial formation of crystalline assemblies (3 h), the gradual disappearance of fibrils up to 72 h (during which time the tyrosine fluorescence increases), and finally the presence of crystals only. At this point, there are no further changes in fluorescence or hence in the environment of the tyrosine residue. Other concentrations ranging from 0.5 to 10 mg/mL were explored and showed a similar correlation between intrinsic fluorescence and morphology (data not shown).

Tyrosine is more easily quenched and more solvent-exposed in fibers than in crystals

Various agents can be used to quench the fluorescence of a fluorophore and give further information on the extent to which that residue is accessible to solvent. Acrylamide was used previously to quench tyrosine fluorescence (33,34), and was used here to generate a Stern-Volmer plot (Fig. S2). K_{sv} values were calculated as 13.6 $\pm$ 0.6 M^{-1} for fibers (present at time 0) and 10.4 $\pm$ 0.1 M^{-1} for crystals (present

at 168 h). Higher K_{sv} values suggest that tyrosine is more readily quenched and is therefore more solvent-accessible in fibers than in crystals, in agreement with the intrinsic fluorescence data.

LD supports a cross-β structure and reveals a change in the orientation of the tyrosine residue over time

LD has the potential to report directional information regarding the orientation of the peptide backbone and the side chains in both fiber and crystal states and as a function of time. To examine the spectra arising from the backbone orientation of the GNNQQNY peptide in crystals, we diluted preincubated peptide 10-fold at a concentration of 2 mg/mL. This was necessary to reduce the high absorbance and light scattering at low wavelength that left insufficient light intensity at the detector below ~215 nm (Fig. 2 *a*). The spectra were taken while the solution was rotated in a Couette cell so that the long axes of the crystals were oriented with the direction of flow. These data show a dominant backbone transition for the β-structure at ~195 nm (35) arising from a transition dipole moment that is oriented perpendicular to the β-strands. This is consistent with the cross-β structure shown previously (35). The LD signal in the aromatic region (Fig. 2 *b*) shows two maxima at 278 nm and 286 nm. This is evidence of exciton coupling of the tyrosine residues, which occurs when the tyrosines are in close proximity. The positive signals appearing at the same time, at ~230–240 nm, are also consistent with exciton coupling of the tyrosine residues (36).

LD was then used to examine the development of these features during the fiber formation process. To allow direct comparison with other kinetic data collected in this study, the peptide was not diluted and rotated in a Couette cell to induce alignment. This prevented LD data from being recorded in the far-UV region (due to absorbance and light scattering), so instead only the signals in the n-π* (very low intensity for β-sheets) and aromatic regions were measured (>215 nm). In the kinetics experiment (Fig. 2 *b*), the presence of an increasing LD signal over time means that the fibers/crystals are growing and/or aligning more effectively. The increased light scattering over time (as observed by the increase in the baseline signal outside the wavelength where there are absorbance bands (300–320 nm)) is indicative of an increase in the size and/or number of the particles in the sample, consistent with fiber and/or crystal growth. The presence of an aromatic LD signal at ~280 nm indicates that the tyrosine residues are ordered within the fibers and crystals. The transitions for tyrosine are illustrated in Fig. 2 *c*. Furthermore, there is a change in the sign of the aromatic LD signal over time (when the sloping baseline due to light scattering is taken into consideration; Fig. 2 *b*, *inset*), indicating that the tyrosine side chain changes its orientation early in the kinetics process.

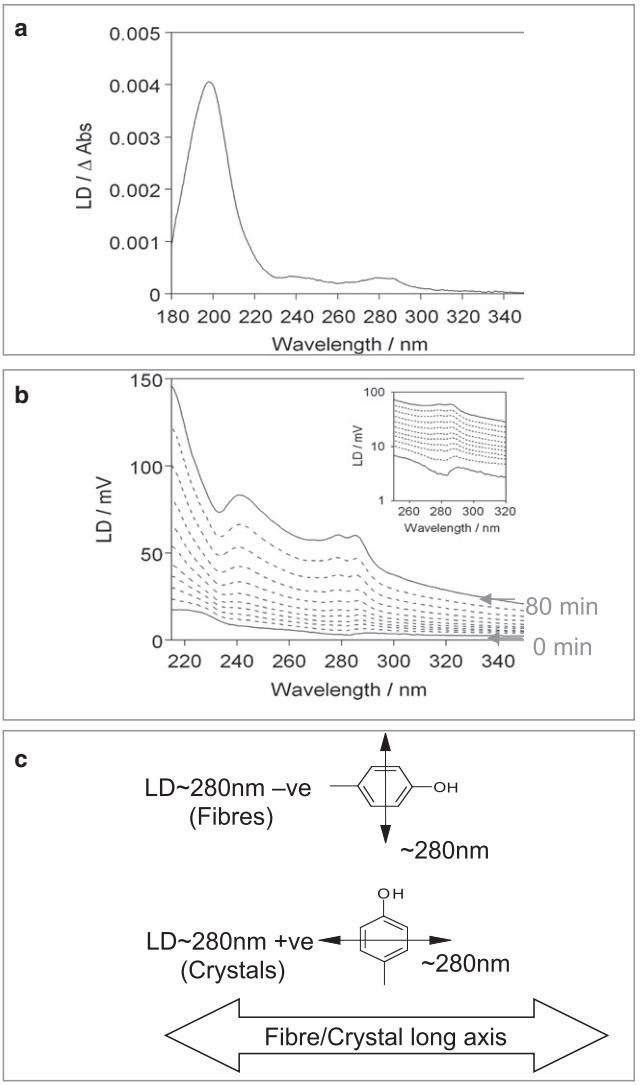

FIGURE 2 (*a*) LD spectrum of mature G1 peptide sample at 0.2 mg/mL. A strong π-π* transition at ~195 nm is consistent with the formation of cross-β structure. There are aromatic signals at ~280 nm resulting from ordered tyrosine side chains in the structure. (*b*) Kinetics of fiber/crystal formation by G1 peptide at 2 mg/mL. Spectra were measured at 8 min intervals. The inset shows the aromatic region plot on a log scale showing the inversion of the aromatic signal at early time points. Units are in millivolts, as explained in Materials and Methods. (*c*) Direction of the transitions that give rise to the LD signals observed in the near-UV region for fibers and crystals.

Experimental and calculated fiber diffraction analyses of GNNQQNY fibers and crystals imply structural differences between fibers and crystals

Diffraction patterns from partially aligned fibrils and crystal preparations of GNNQQNY were collected and revealed the expected cross-β patterns (Fig. 3) with a strong meridional reflection at 4.7 Å. Of interest, the three patterns collected gave slightly different positions of equatorial diffraction signals (Table 1) and had different reflections on the equator (19 Å in the crystals, and 31.3 Å and 13.7 Å in the fibers),

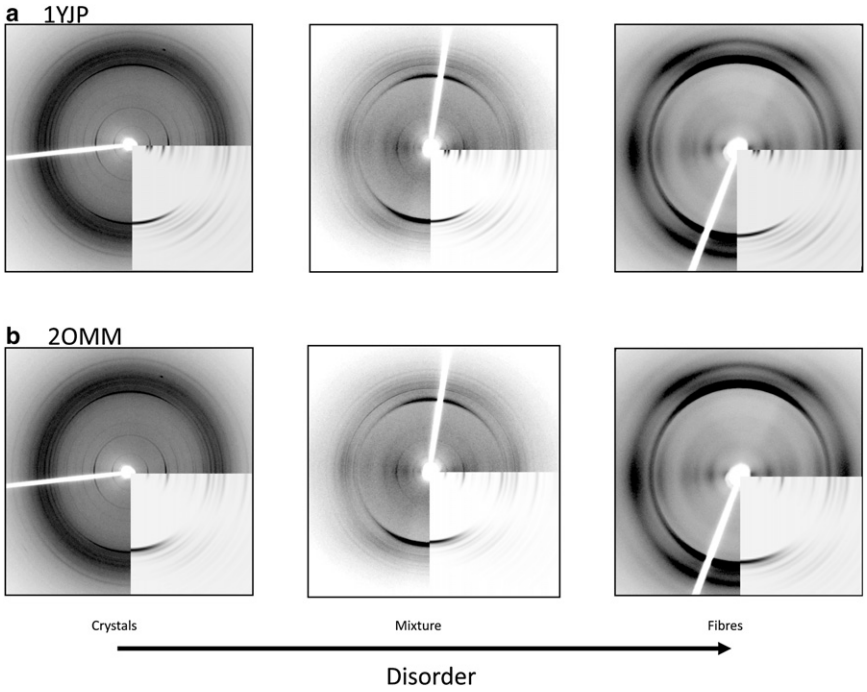

FIGURE 3 Comparison of experimental and simulated fiber diffraction patterns. Simulations are shown in the bottom right-hand corner of each image and were calculated to correspond to the experimental diffraction settings. Fiber axis is vertical. Crystalline, mixed fibers and crystals, and fibrillar samples are compared with simulated diffraction patterns from the crystal structure of (*a*) 1yjp and (*b*) 2omm.

suggesting that their internal architecture varies. Strong reflections at ~10–11 Å on the equator often arise from the sheet spacings, whereas the low-angle reflections are from the chain length, or the width of the protofilaments. A comparison between the signal positions from the three preparations suggests that the positions of the reflections are combined in the preparation known to contain a mixture of both fibers and crystals.

To relate the GNNQQNY preparations with the published crystal structure, we calculated the diffraction patterns from the crystal structure coordinates, 1yjp and 2omm (Fig. S2). These structures crystallize in different unit cells and space groups (13,14), giving rise to different packing of the peptide chains and environments of the tyrosine residue. The 1yjp structure has a very wide separation of sheets at the wet interface, with a spacing of ~15 Å. The position of the meridional reflections arising from the hydrogen bonding between β-strands differs between the two structures (Table 2 and Fig. S1) and the equatorial positions show clear differences that are likely to arise from the different packing arrangements. A close examination and comparison of the experimental and calculated diffraction patterns (Fig. 3) shows a reasonable match between the equatorials of the experimental pattern from crystalline fibers and mixed preparations with the calculated pattern from the 2omm structure (Fig. 3 *b*). In the 1yjp pattern, the positions of the equatorial reflections are not similar to experimental data. Of interest, the equatorial reflections in the diffraction pattern from fibrils do not match either calculated pattern well (in particular, the strong 13.7 Å reflection is missing in both), which may indicate that fibers rearrange structurally to become crystals, consistent with our other data.

TABLE 1 Comparison of reflection positions measured from experimental diffraction patterns (only the most intense reflections are shown)

	Crystals	Mixture	Fibers
Equatorial reflections (Å)			31.3
	19.7	19.3	
		13.7	13.7
	9.9	9.9	9.2
	7.4	7.4	7.9
Meridional reflections (Å)	4.75	4.72	4.75

DISCUSSION

The relationship between the structures of crystals and amyloid-like fibrils formed from the peptide GNNQQNY has been studied previously (13–17), and it has been proposed that the crystals share many structural similarities

TABLE 2 Comparison of reflection positions measured from fiber diffraction patterns calculated from monoclinic and orthorhombic crystal coordinates (only the most intense reflections are shown)

	1yjp	2omm
Equatorial reflections (Å)	22.6	
		19.6
	18.0	
	11.2	11.5
	8.9	9.3
		5.5
Meridional reflection (Å)		4.85
Meridional reflection (Å)	4.75	

with the fibrils (14). Here, we present data that suggest that although there are some fundamental structural similarities between fibers and crystals, there are also some important differences. We probed the structural environment of the tyrosine residue and found that the tyrosine exists in a different conformation in the crystals compared to the fibers. The assembly of crystals is preceded by fibril formation, and the gradual disappearance of fibrillar material formed from the peptide GNNQQNY, as well as the increasing width of ribbons and crystals as observed by EM, could be explained in two possible ways. The fibers may be laterally associating in some manner to form the crystals, or, more likely, there may be a separate pathway that leads to the formation of crystals, possibly involving fragmentation or monomer dissociation of the fibrils. In either case, it is possible that some structural rearrangement is taking place as the crystals form, and that this crystal form is the most stable arrangement. This was the basis for our further investigations.

The comparatively lower intensity in tyrosine fluorescence observed for fibrils compared to crystals implies that the tyrosine residues are significantly more solvent-exposed in the fibrils, either because they are located on the surface or because they are exposed to solvent present within the structure. This result is corroborated by the K_{sv} values obtained for fibers and crystals calculated from acrylamide quenching experiments. The tyrosine residue is located at the C-terminus, and therefore burial of the tyrosine as crystals form might be expected. This is consistent with the observed increase in fluorescence intensity accompanying the observed morphological changes from narrow fibrils to crystals. However, this change in solvent exposure does not preclude the possibility that the tyrosine residues may also be undergoing structural rearrangements as they participate in these different species, or that their mobility may drive the formation of polymorphisms in the fibrils. The data from acrylamide quenching experiments can be fitted to a straight line (see Fig. S2), consistent with simple collision quenching taking place.

From our EM results, we know that fibers are formed immediately on dissolution of peptide with water, and we can therefore assume that the LD signal at time 0 is specific to fibrillar material. At the end of the LD experiment, crystals are observed in electron micrographs, and the final LD signal is different from that of the fibrillar material. The flow that the peptide experiences in the Couette cell is likely responsible for the crystals forming more quickly than in other experiments (37). The change in the near-UV signal over time at ~280 nm can only be due to a change in the orientation of the tyrosine residue: in the fibers it has one orientation with respect to the fiber axis, whereas in crystals it has another.

The observed splitting of the 280 nm tyrosine peak suggests coupling of the tyrosine residues, which would be the case if they were in close proximity. This proximity could arise either from stacking in the hydrogen-bonding direction, or possibly from interactions between sheets.

The transition moment that gives rise to the signals at ~280 nm in tyrosine is illustrated in Fig. 2 *c*. Thus, in fibers the tyrosine residue is oriented such that, on average, the transition moment shown is pointing more perpendicular than parallel to the fiber long axis. In crystals, the tyrosine transition moment that absorbs at ~280 nm is oriented more parallel to the crystal long axis, giving rise to a positive LD signal in this region (Fig. 2 *c*). Given that for fibers and crystals (which have rotational symmetry about the long axis),

$$\mathrm{LD} = \frac{3}{2}S\left(3\cos^2\alpha - 1\right),$$

where α is the angle between the fiber (or crystal axis) and the 280 nm transition polarization, and S is the degree of orientation, a positive signal means that the transition moment is $<54.7^\circ$ from the alignment axis (fiber/crystal long axis) and a negative signal means that this angle is $>54.7^\circ$. It is important to note the sloping baseline that is seen in these spectra is indicative of large structures scattering the light. Thus, when we refer to a negative signal in this context, we mean a signal that drops below this sloping baseline. It is possible in some cases to correct for this light scattering; however, when the particles that are scattering the light are large (relative to the wavelength of the light), the scattering becomes complex (Mie scattering), and this process can introduce artifacts into the data. For this reason, we did not process the data to correct for light scattering.

Fiber diffraction analysis suggests that the packing of the GNNQQNY peptides within the initially formed fibrils may differ from the published crystal structures, and that rearrangements take place accompanying the conversion to crystals. This could be a conversion from a possibly hydrated wider sheet spacing in the fibrils to a steric zipper arrangement with a dry interface in the crystals. This is seen in the gradual change in the diffraction patterns from fibers, to mixtures of crystals and fibers to the final crystals, and from our other results that suggest that this rearrangement may involve changes in the orientation of the tyrosine. It is even conceivable from this and other work (18) that such aromatic interactions may be a driving force for these changes to take place. Aromatic residues feature in many amyloid-forming proteins (e.g., FF pairs in Aβ and serum amyloid protein), and their presence may play an important role in assembly and/or structural stability. In addition, our analysis indicates that the crystals that form under the conditions used here are consistent with the crystal structure represented by the orthorhombic crystal form (14) (Fig. 3 *b* and Tables 1 and 2).

CONCLUSIONS

Our results suggest that GNNQQNY initially forms fibers and then crystals. The pathway by which this occurs is

unclear, but we propose that it is either by lateral association of fibers or, more likely, by fragmentation of existing fibers being replaced by crystal nuclei. In all concentrations tested, we noted that the formation of crystals was favored as time proceeded, indicating that crystals are the most stable species. In this work, we used the fluorescent characteristics of the tyrosine residue to monitor assembly. Tyrosine is more buried in fibers than in crystals, suggesting a change in its environment between the two species. LD and fiber diffraction data report that the two species are structurally distinct in terms of both peptide chain packing and the position of the tyrosine residue. LD enables the tyrosine transition to be followed as a function of time, and fiber diffraction analysis indicates that the fibrils may be structurally different from either crystal structure, whereas crystals show similarities to the orthorhombic crystal structure for GNNQQNY. These results may suggest the importance of aromatic interactions in the assembly of fibrils and crystals, and their potential role in driving the formation of different structural species. In addition, the work presented here highlights the structural variations that may exist between these species (i.e., fibers and crystals), and the important implications these differences will have in their characterization.

SUPPORTING MATERIAL

Two figures are available at http://www.biophysj.org/biophysj/supplemental/S0006-3495(09)01627-0.

The authors thank Julian Thorpe for help with the electron microscopy, and Cedric Dicko for help with the LD analysis.

L.S. received funding from the Biotechnology and Biological Sciences Research Council and Alzheimer's Research Trust, and a donation from Michael Chowen. M.H. and A.R. received funding from the Engineering and Physical Sciences Research Council and the Biotechnology and Biological Sciences Research Council. S.V.H. received funding from the Danish Council for Independent Research | Natural Sciences, and the Lundbeck Foundation.

REFERENCES

1. Pepys, M. B. 2006. Amyloidosis. *Annu. Rev. Med.* 57:223–241.
2. Geddes, A. J., K. D. Parker, …, E. Beighton. 1968. "Cross-β" conformation in proteins. *J. Mol. Biol.* 32:343–358.
3. Serpell, L. C., M. Sunde, and C. C. Blake. 1997. The molecular basis of amyloidosis. *Cell. Mol. Life Sci.* 53:871–887.
4. Makin, O. S., and L. C. Serpell. 2005. Structures for amyloid fibrils. *FEBS J.* 272:5950–5961.
5. Westermark, P., M. D. Benson, …, J. D. Sipe. 2007. A primer of amyloid nomenclature. *Amyloid.* 14:179–183.
6. Tycko, R. 2004. Progress towards a molecular-level structural understanding of amyloid fibrils. *Curr. Opin. Struct. Biol.* 14:96–103.
7. White, H. E., J. L. Hodgkinson, …, H. R. Saibil. 2009. Globular tetramers of β (2)-microglobulin assemble into elaborate amyloid fibrils. *J. Mol. Biol.* 389:48–57.
8. Vilar, M., H. T. Chou, …, R. Riek. 2008. The fold of α-synuclein fibrils. *Proc. Natl. Acad. Sci. USA.* 105:8637–8642.
9. Sachse, C., M. Fändrich, and N. Grigorieff. 2008. Paired β-sheet structure of an Aβ (1-40) amyloid fibril revealed by electron microscopy. *Proc. Natl. Acad. Sci. USA.* 105:7462–7466.
10. Ding, T. T., and J. D. Harper. 1999. Analysis of amyloid-β assemblies using tapping mode atomic force microscopy under ambient conditions. *Methods Enzymol.* 309:510–525.
11. Makin, O. S., P. Sikorski, and L. C. Serpell. 2006. Diffraction to study protein and peptide assemblies. *Curr. Opin. Chem. Biol.* 10:417–422.
12. Marshall, K. E., and L. C. Serpell. 2009. Structural integrity of β-sheet assembly. *Biochem. Soc. Trans.* 37:671–676.
13. Nelson, R., M. R. Sawaya, …, D. Eisenberg. 2005. Structure of the cross-β spine of amyloid-like fibrils. *Nature.* 435:773–778.
14. Sawaya, M. R., S. Sambashivan, …, D. Eisenberg. 2007. Atomic structures of amyloid cross-β spines reveal varied steric zippers. *Nature.* 447:453–457.
15. Balbirnie, M., R. Grothe, and D. S. Eisenberg. 2001. An amyloid-forming peptide from the yeast prion Sup35 reveals a dehydrated β-sheet structure for amyloid. *Proc. Natl. Acad. Sci. USA.* 98:2375–2380.
16. Diaz-Avalos, R., C. Long, …, D. L. Caspar. 2003. Cross-β order and diversity in nanocrystals of an amyloid-forming peptide. *J. Mol. Biol.* 330:1165–1175.
17. van der Wel, P. C., J. R. Lewandowski, and R. G. Griffin. 2007. Solid-state NMR study of amyloid nanocrystals and fibrils formed by the peptide GNNQQNY from yeast prion protein Sup35p. *J. Am. Chem. Soc.* 129:5117–5130.
18. Gazit, E. 2002. A possible role for π-stacking in the self-assembly of amyloid fibrils. *FASEB J.* 16:77–83.
19. Esposito, L., C. Pedone, and L. Vitagliano. 2006. Molecular dynamics analyses of cross-β-spine steric zipper models: β-sheet twisting and aggregation. *Proc. Natl. Acad. Sci. USA.* 103:11533–11538.
20. Berryman, J. T., S. E. Radford, and S. A. Harris. 2009. Thermodynamic description of polymorphism in Q- and N-rich peptide aggregates revealed by atomistic simulation. *Biophys. J.* 97:1–11.
21. Maji, S. K., J. J. Amsden, …, D. B. Teplow. 2005. Conformational dynamics of amyloid β-protein assembly probed using intrinsic fluorescence. *Biochemistry.* 44:13365–13376.
22. Padrick, S. B., and A. D. Miranker. 2002. Islet amyloid: phase partitioning and secondary nucleation are central to the mechanism of fibrillogenesis. *Biochemistry.* 41:4694–4703.
23. Kirkitadze, M. D., M. M. Condron, and D. B. Teplow. 2001. Identification and characterization of key kinetic intermediates in amyloid β-protein fibrillogenesis. *J. Mol. Biol.* 312:1103–1119.
24. Sreerama, N., M. C. Manning, …, R. W. Woody. 1999. Tyrosine, phenylalanine, and disulfide contributions to the circular dichroism of proteins: circular dichroism spectra of wild-type and mutant bovine pancreatic trypsin inhibitor. *Biochemistry.* 38:10814–10822.
25. Bhattacharjee, S., G. Tóth, …, J. D. Hirst. 2003. Influence of tyrosine on the electronic circular dichroism of helical peptides. *J. Phys. Chem. B.* 107:8682–8688.
26. Rodger, A., and B. Nordén. 1997. Circular Dichroism and Linear Dichroism. Oxford University Press, Oxford, UK.
27. Abramoff, M. D., P. J. Magelhaes, and S. J. Ram. 2004. Image Processing with Image. *J. Biophotonics Int.* 11:36–42.
28. Lakowicz, J. R. 1999. Principles of Fluorescence Spectroscopy, 2nd ed. Kluwer Academic/Plenum, London, UK.
29. Rodger, A., R. Marrington, …, T. R. Dafforn. 2006. Looking at long molecules in solution: what happens when they are subjected to Couette flow? *Phys. Chem. Chem. Phys.* 8:3161–3171.
30. Dicko, C., M. R. Hicks, …, S. V. Hoffmann. 2008. Breaking the 200 nm limit for routine flow linear dichroism measurements using UV synchrotron radiation. *Biophys. J.* 95:5974–5977.

31. Zibaee, S., O. S. Makin, …, L. C. Serpell. 2007. A simple algorithm locates β-strands in the amyloid fibril core of α-synuclein, Aβ, and τ using the amino acid sequence alone. *Protein Sci.* 16:906–918.

32. Madine, J., E. Jack, …, D. A. Middleton. 2008. Structural insights into the polymorphism of amyloid-like fibrils formed by region 20–29 of amylin revealed by solid-state NMR and X-ray fiber diffraction. *J. Am. Chem. Soc.* 130:14990–15001.

33. Padrick, S. B., and A. D. Miranker. 2001. Islet amyloid polypeptide: identification of long-range contacts and local order on the fibrillogenesis pathway. *J. Mol. Biol.* 308:783–794.

34. Dusa, A., J. Kaylor, …, A. L. Fink. 2006. Characterization of oligomers during α-synuclein aggregation using intrinsic tryptophan fluorescence. *Biochemistry.* 45:2752–2760.

35. Dafforn, T. R., J. Rajendra, …, A. Rodger. 2004. Protein fiber linear dichroism for structure determination and kinetics in a low-volume, low-wavelength couette flow cell. *Biophys. J.* 86:404–410.

36. Khan, M. A., C. Neale, …, R. E. Bishop. 2007. Gauging a hydrocarbon ruler by an intrinsic exciton probe. *Biochemistry.* 46:4565–4579.

37. Hill, E. K., B. Krebs, …, D. E. Dunstan. 2006. Shear flow induces amyloid fibril formation. *Biomacromolecules.* 7:10–13.